Title: Proper control of R-loop homeostasis is required for maintenance of gene expression and neuronal function during aging

Running title: R-loop dysregulation in the aging eye

Authors: Juan Jauregui-Lozano[1], Spencer Escobedo[1], Alyssa Easton[2], Nadia A. Lanman[3,4], Vikki M. Weake[1,4] and Hana Hall[1,5]

[1] Department of Biochemistry, Purdue University, West Lafayette, Indiana

[2] Department of Agricultural and Biological Engineering, Purdue University, West Lafayette, Indiana

[3] Department of Comparative Pathobiology, College of Veterinary Medicine, Purdue University, West Lafayette, IN.

[4] Purdue University Center for Cancer Research, Purdue University, West Lafayette, Indiana

[5] Purdue Institute for Integrative Neuroscience, Purdue University, West Lafayette, IN.

Correspondence

Hana Hall, Department of Biochemistry, Purdue University, 175 S. University Street, West Lafayette, IN 47907, USA, Email: hallh@purdue.edu

Funding information: Research reported in this publication was supported by the National Eye Institute of the NIH under Award Number 1R21EY031024-01 (to V.M.W. and H.H.) and 2R01EY024905 to V.M.W.

ABSTRACT

Age-related loss of cellular function and increased cell death are characteristic hallmarks of aging. While defects in gene expression and RNA metabolism have been linked with age-associated human neuropathies, it is not clear how the changes that occur in aging neurons contribute to loss of gene expression homeostasis. R-loops are RNA-DNA hybrids that typically form co-transcriptionally via annealing of the nascent RNA to the template DNA strand, displacing the non-template DNA strand. Dysregulation of R-loop homeostasis has been associated with both transcriptional impairment and genome instability. Importantly, a growing body of evidence links R-loop accumulation with cellular dysfunction, increased cell death and chronic disease onset. Here, we characterized the R-loop landscape in aging *Drosophila melanogaster* photoreceptor neurons and showed that bulk R-loop levels increased with age. Further, genome-wide mapping of R-loops revealed that transcribed genes accumulated R-loops over gene bodies during aging, which correlated with decreased expression of long and highly expressed genes. Importantly, while photoreceptor-specific down-regulation of Top3β, a DNA/RNA topoisomerase associated with R-loop resolution, lead to decreased visual function, overexpression of Top3β or nuclear-localized RNase H1, which resolves R-loops, enhanced positive light response during aging. Together, our studies highlight the functional link between dysregulation of R-loop homeostasis, gene expression and visual function during aging.

KEYWORDS: *Drosophila*, eye, aging, R-loop, transcription, visual, photoreceptors, neurons.

48 **1 INTRODUCTION**

49 Aging is a process characterized by a time-dependent decline in physiological homeostasis that
50 eventually leads to a loss of organismal function and increased incidence of death.
51 Characteristic functional changes include loss of gene and protein expression, mitochondrial
52 dysfunction, cellular senescence, and stem cell exhaustion (López-Otín et al., 2013). Aging is
53 also a major contributor to development of many chronic diseases including ocular disease
54 (Bonnel et al., 2003). Age-related vision loss and maculopathy have been associated with
55 decreased density of retinal cells, including photoreceptors. Specifically, the age-related decline
56 in photoreceptors affects predominantly rods rather than cones (Jackson et al., 2002). In
57 addition, emerging evidence links age-related neurological diseases, including retinal
58 neuropathies, to defects in gene expression and RNA metabolism (Parapuram et al., 2010).
59 Nonetheless, the molecular mechanisms that contribute to the age-associated susceptibility of
60 the eye to disease development are poorly understood.

61 R-loops are three-stranded nucleic acid structures consisting of an RNA-DNA hybrid and a
62 misplaced single strand of DNA (Aguilera & García-Muse, 2012). They typically form during
63 transcription in organisms ranging from yeast to humans and play a significant role in normal
64 cellular physiology, being required for the initiation of mitochondrial replication and class switch
65 recombination. Notably, recent studies suggest that R-loops can dynamically regulate gene
66 expression (Niehrs & Luke, 2020); for example, due to their enrichment at gene termini, R-loops
67 can modulate gene expression by preventing DNA methylation or limiting transcription factor
68 access to promoters and facilitating efficient transcription termination at 3'-ends (Boque-Sastre
69 et al. 2015; Skourti-Stathaki et al. 2014). Moreover, R-loop formation correlates positively with
70 active transcription, gene length, GC content and DNA topology (Mackay et al., 2020).
71 Importantly, recent studies have shown that resolution of topological stress during transcription
72 mediated by topoisomerases is critical for proper neuronal function (McKinnon, 2016).

73 Topoisomerase 3β (Top3β) is a member of the type IA superfamily of topoisomerases, which
74 unwind negatively supercoiled DNA formed during transcription and replication, an activity that
75 prevents R-loop formation (Mackay et al., 2020). Loss of Top3β is associated with neurological
76 disorders (Mackay et al., 2020) and has been shown to reduce lifespan in mice (Kwan & Wang,
77 2001).

78 Although R-loops are normal biological structures, their persistent formation is a major source of
79 spontaneous DNA damage that can lead to transcriptional dysregulation and genome instability
80 (Aguilera & García-Muse, 2012); two early hallmarks of aging. Given that aging is a main risk
81 factor for development of chronic diseases, including neurodegenerative disease, it is
82 conceivable that R-loops could play a significant role in age-associated mis-regulation of cellular
83 functions. However, our understanding on R-loop biology during aging, and particularly in
84 neurons, is quite limited. Due to high levels of transcription and alternative splicing, retinal cells
85 and particularly photoreceptor neurons may be highly sensitive to RNA metabolism
86 dysregulation. *Drosophila* compound eye contains approximately 800 units called ommatidia
87 with each consisting of 20 cells, including eight photoreceptor (PR) neurons. The six outer PRs
88 (R1-R6) expressing Rhodopsin 1 (Rh1) are mainly responsible for black and white vision and
89 motion, and are similar to human rods. The inner PRs (R7 and R8) express Rh3/4 and Rh5/6,
90 respectively, are responsible for color vision and resemble human cones. To characterize how
91 aging impacts the genomic R-loop landscape in *Drosophila* photoreceptors, we isolated
92 genetically labeled outer PRs using our recently improved nuclei immuno-enrichment method
93 (Jauregui-Lozano et al., 2021) and performed MapR coupled with next generation sequencing
94 (Yan & Sarma, 2020). Here, we show that R-loop levels in photoreceptor neurons increased
95 progressively with age and were associated with genic characteristics, such as transcript levels
96 and GC content. Further, our data show that majority of genes that decrease expression during
97 aging contained R-loops. Finally, photoreceptor-specific depletion of DNA/RNA topoisomerase

98 Top3β resulted in increased R-loop levels, reduced expression of long genes with neuronal
99 function and reduced visual response. Importantly, overexpression of either Top3β or human
100 RNASEH1, an enzyme that resolves R-loops, in the eyes resulted in enhanced visual response
101 during aging. Together, our data show that aging is associated with increased levels of R-loops
102 over transcribed genes, potentially disrupting transcriptional outcomes that contribute to age-
103 associated changes in neuronal function, including visual response to light.

104 **2 RESULTS**

105 **2.1 Aging photoreceptor neurons show increased global R-loop levels that correlate with**
106 **loss of function and precede age-associated retinal degeneration**

107 To examine the global R-loop levels in photoreceptor neurons, we tagged the outer nuclear
108 membrane of R1-R6 with GFP fused to the KASH domain of Msp300 protein using the Rh1-
109 Gal4 driver and isolated outer PR nuclei from the head homogenate with our tissue-specific
110 method (Jauregui-Lozano et al., 2021). Next, we aged flies over the course of 50 days post-
111 eclosion (emergence from the pupae) and extracted genomic DNA from isolated PR nuclei at
112 three time points (Figure 1A). We then assessed the global R-loop signal with a DNA slot blot
113 assay using the S9.6 antibody, which recognizes RNA-DNA hybrids. Specificity of S9.6 antibody
114 towards RNA-DNA hybrids was shown by pre-treatment of DNA with ribonuclease H1 (RNase
115 H1) that resulted in significant decrease of S9.6 signal (Figure 1B). Signal quantification showed
116 approximately 30% increase in R-loop levels in PRs isolated from middle-aged, 30-day old flies
117 as compared to that in young, 10-day old flies. This trend continued with a significant increase
118 of nearly 50% in global R-loop levels at day 50 (Figure 1B-C). These data show that R-loops
119 start accumulating early during photoreceptor aging, at a time point where flies show decreased
120 visual function (Hall et al., 2017). Importantly, using optical neutralization, which measures
121 photoreceptor structural integrity with light microscopy, we observed no retinal degeneration by
122 middle age, with a stochastic loss of rhabdomeres occurring after day 40 (Figure S1). Thus, our

123 data show that process of R-loop accumulation precedes age-related retinal degeneration, thus
124 suggesting that increased R-loop formation may contribute to loss of function and possibly
125 neuronal cell loss during aging.

126 **2.2 Profiling genome-wide R-loop distribution in PR neurons reveals age-associated**
127 **changes**

128 To determine the genomic R-loop landscape in aging PRs, we coupled our NIE approach with
129 MapR, a recently published R-loop mapping strategy based on the specificity of RNase H1
130 enzyme to RNA-DNA hybrids, combined with the micrococcal nuclease (MNase)-based
131 CUT&RUN technology. MapR uses a recombinant mutant form of MNase-fused RNase H1,
132 which binds but does not degrade the RNA moiety within an RNA-DNA hybrid (ΔRH). Upon
133 binding of the RNA-DNA hybrid by ΔRH-MNase, MNase activation by Ca^{2+} addition results in
134 cleavage of surrounding DNA and a subsequent release of R-loop associated DNA fragment,
135 which is used for library preparation coupled with high-throughput sequencing (Figure 2A).
136 Surprisingly, we found that coupling NIE-purified photoreceptor nuclei with the standard MapR
137 protocol yielded signal over genic regions resembling MNase-seq rather than R-loop specific
138 enrichment. Our data showed MapR signal depletion around the Transcription Start Site (TSS)
139 of genic regions (Figure S2A), suggesting that our samples were being over-digested by
140 MNase. We therefore modified the standard MapR protocol based on the recently published
141 improvement of the CUT&RUN method, which incorporates high salt with low calcium washing
142 steps, and also decreased digestion time (see Methods in Supporting Information). To evaluate
143 the quality of our modified protocol, we first compared our MapR data in *Drosophila* PRs to the
144 original MapR data obtained in human HEK293T cells (Figure S2B) and found that the
145 metagene profiles over the gene bodies showed similar R-loop distribution, with signal
146 enrichment around the TSS and the Transcription Termination Site (TTS) (Figure S2A). In
147 contrast, when we next compared our MapR data with R-loop mapping data obtained from

148 *Drosophila* embryos using DRIP-seq (Alecki et al., 2020), we observed that DRIP-seq showed
149 signal enrichment over gene bodies with a slight depletion around TSS (Figure S2C);
150 discrepancies that have been shown previously to result from different affinities of S9.6 antibody
151 used in DRIP-seq, as opposed to RNase H1 used in MapR, for RNA-DNA hybrids. In addition,
152 the Alecki dataset was obtained during *Drosophila* early embryonic developmental stages.
153 Thus, some differences in signal enrichment in our studies might arise from tissue-specific and
154 method-specific effects.

155 To validate the specificity of our MapR method, we treated NIE-purified PR nuclei with RNase-
156 H1 prior to performing MapR, which led to a complete loss of signal enrichment as shown by
157 individual gene examples (Figure 2B) and gene metaplots (Figure 2C). In addition, when we
158 normalized MapR signal by obtaining a ratio from RNaseH1 non-treated relative to treated
159 samples, we found that the MapR signal distribution did not show significant changes in
160 enrichment over genes bodies (Figure S2D). We note that the standard MapR protocol includes
161 a separate negative control where nuclei are incubated with MNase alone to account for MNase
162 binding. However, in our hands, the MNase control yielded no purifiable DNA, as shown by
163 TapeStation profiles (Figure S2E).

164 Based on these observations, we performed MapR in aging PRs at day 10, 30 and 50 post-
165 eclosion using our modified approach in three independent biological replicates which
166 generated at least $3.5x10^7$ uniquely mapped fragments per sample (Supplemental File 1).
167 Spearman's correlation analysis based on read distribution over a 1000-bp binned genome
168 revealed a strong positive association amongst the three biological replicates (Spearman's $p \geq$
169 0.96). In contrast, when we compared the samples between different age time points, we
170 observed lower positive association between day 10 and day 50 (Spearman's $p \geq 0.93$),
171 suggesting that the R-loop landscape changes were age-dependent (Figure 2D). Similarly,
172 Principal Component Analysis (PCA) of the normalized R-loop distribution revealed that 53.8%

173 variance amongst the samples for all biological replicates was attributed to age (Figure 2E).
174 Notably, while samples clustered by age, the similarity amongst the biological replicates
175 decreased with age (PC2 13.6%), suggesting that aging is associated with increased
176 heterogeneity in R-loop distribution.

177 To further assess the quality of our sequencing datasets, we performed peak calling using the
178 Model-based Analysis for ChIP-Seq (MACS2) algorithm using default settings and measured
179 quality control metrics. To account for the differences in the number of mapped fragments in
180 each sample (Figure S2F), we called the peaks using bam files that were down-sampled to the
181 same number of mapped fragments ($3.5x10^6$). Evaluation of the Fraction of Reads in Peaks
182 (FRiP) score, which measures the quality of signal enrichment as defined by modENCODE,
183 showed consisted FRiP scores higher than 0.37 for all samples (Figure S2G). Furthermore, we
184 found that peak distribution was stably maintained during aging, with approximately 60% of
185 peaks being annotated to promoters (TSS ± 2kb) and approximately 25% of peaks annotated to
186 introns (Figure S2H), which is consistent with previously reported genome-wide R-loop
187 distribution.

188 Taken together, our data demonstrate that we successfully applied the MapR method to tissue-
189 specific samples in *Drosophila,* by purifying photoreceptor nuclei from the whole organism, and
190 produced high quality R-loop mapping data. Furthermore, application of MapR in aging PRs
191 showed that the genome-wide R-loop distribution changes in an age-dependent manner.

192 **2.3 Age-associated R-loop accumulation over gene bodies correlates with high GC**
193 **content, gene length and transcriptional levels**

194 Given that R-loops typically form co-transcriptionally (Belotserkovskii et al., 2018), we next
195 examined global and locus-specific distribution of age-associated changes in R-loops across
196 actively transcribed genes, defined as having more than seven transcripts per million (TPM).

197 First, we analyzed global R-loop signal over gene bodies for actively expressed genes and
198 compared the average signal across the gene, as counts per million (CPM). As expected, gene
199 metaplots revealed that R-loop signal was enriched mainly over TSS and towards the 3' ends of
200 genes across all age time points (Figure 3A), which is consistent with previously reported R-loop
201 distribution (Ginno et al. 2012; Sanz et al. 2016a; Nadel et al. 2015; Chen et al. 2017).
202 Importantly, there was a widespread increase in R-loop levels over gene bodies during aging,
203 most notably at day 50. Genome browser inspection of the averaged signal tracks for each time
204 point for two individual genes showed changes in R-loop signal, including an early decrease or
205 late increase (Figure S3A). To further evaluate the molecular characteristics of R-loop coverage
206 during aging, we asked whether the age-associated increase in R-loops could be a
207 consequence of broadening of the peaks. Consistent with our gene metaplots, MapR signal
208 around the peaks showed that overall, R-loop coverage increased with age (Figure 3B),
209 suggesting that R-loops might either extend or form at higher rate with age. To further assess
210 an age-associated increase in R-loop occupancy, we quantified signal coverage, as defined by
211 the sum of peak width for each time point. Notably, R-loop peaks covered approximately 18.7
212 megabases (Mb) of the genome at day 50, compared to 18.1 Mb at day 10, showing a modest
213 but significant increase in coverage during aging (t-test, $p<0.022$) (Figure 3C). Supporting this
214 data, violin plots depicting the peak width for all peaks revealed a slight but consistent increase
215 in peak width at day 30 and day 50 as compared to that at day 10 (Figure S3C). Taken together,
216 these observations show that R-loop signal over the genome accumulates with age,
217 corroborating our findings from bulk R-loop levels using slot blots (see Figure 1). We note that
218 the *Drosophila* genome has a total size of 180 Mb, and our data in *Drosophila* PRs showed that
219 R-loops covered approximately 10% of the genome, which is similar to the genomic R-loop
220 coverage obtained from other organisms, including mammals (Aguilera & García-Muse, 2012).

221 To gain further insight into age-associated changes in R-loops, we compared the fold change in
222 R-loop signal around TSS (±3 kb) or TTS (±3 kb) in old and young PRs. Heatmap plots of
223 actively expressed genes ranked based on their fold change showed that the majority of the
224 TSS-associated R-loops increased with age, while only approximately 50% of genes had an
225 increase in R-loop signal around TTS (Figure 3D). Because R-loop formation is typically
226 associated with specific genic characteristics such as gene expression level, torsional stress,
227 and GC content (Chedin & Benham, 2020), we wondered if such genomic features were
228 associated with an age-associated accumulation of R-loops over actively expressed genes. To
229 test this, we clustered the genes from each heatmap from Figure 3D into four quartiles (Q1-4,
230 with Q1 having the highest R-loop gain and Q4 having the highest R-loops loss), and assessed
231 GC content, gene length and expression levels, respectively. Genes with TSS-enriched R-loops
232 showed higher GC content than genes with R-loop losses (Wilcoxon-test, $p<2.2x10^{-5}$), with no
233 statistically significant association with long or highly expressed genes (Figure 3E-top).
234 However, genes with TTS-enriched R-loops had high GC content, and were highly expressed
235 and long (Kruskal-Wallis, $p<4.5x10^{-2}$, $p<4.5x10^{-4}$, and $p<2.1x10^{-9}$, respectively) (Figure 3E-
236 bottomC). Thus, these data show that age-associated accumulation of R-loops correlates with
237 high GC content, length and expression levels.

238 **2.4 Accumulation of R-loops in long genes correlates with decreased transcript levels in**
239 **aging PRs**

240 We previously showed that genes which decrease expression in aging PRs tend to be highly
241 expressed and longer than genes that either increase or do not change expression (Hall et al.,
242 2017). Moreover, aging *Drosophila* exhibit decrease in positive light response which correlates
243 with decreased expression of long genes with neuronal function. Interestingly, recent reports
244 have shown similar correlations between gene length and function in a variety of aging tissues
245 and organisms, including humans (Lopes et al., 2021; Stoeger et al., 2019). Because our

246 current data showed that long genes accumulated R-loops with age, and R-loops can lead to
247 RNA polymerase II arrest and transcription inhibition (Bentin et al., 2005; Tous & Aguilera,
248 2007), we next investigated if there was an association between accumulation of R-loops and
249 decreased gene expression during aging. Transcriptome profiling of PRs isolated from flies at
250 day 10 and 50 revealed that 1700 genes (18%) were differentially expressed (DEG), with 722
251 genes (7%) decreasing expression and 978 genes (8%) increasing expression (p-adj<0.05,
252 |FC|>1.5) (Figure 4A). To further evaluate the relationship between genic R-loop accumulation
253 and gene expression, we identified R-loop containing genes (RCGs), by annotating high
254 confidence peaks to the nearest TSS, and compared them to DEGs during aging. Venn diagram
255 analysis revealed that 1388, or 69% genes were age-regulated at a transcript level and also
256 contained at least one R-loop (RCGs/DEGs) (Figure 4B). Further, gene length analysis of each
257 category showed that RCG/DEGs were significantly longer than either DEGs or RCGs alone
258 (Figure 4C), suggesting that accumulation of R-loops in long genes could contribute to gene
259 expression changes during aging (Wilcoxon test, adjusted p-value < 2.22e-16).

260 To gain further insight into the biological processes associated with RCG/DEGs, we first used
261 hierarchical clustering and identified 613 genes (46%) to be up-regulated and 775 genes (54%)
262 being down-regulated. Importantly, we found that overall, nearly 80% of the genes that
263 decreased expression during aging accumulated R-loops, while only 58% of the genes that
264 increased expression during aging contained R-loops (Figure 4D). Gene Ontology (GO) term
265 analysis revealed that down-regulated RCG/DEGs were enriched for functional and neuronal
266 categories, including cognition and regulation of nervous system development, whereas up-
267 regulated RCG/DEGs were enriched for metabolic processes, such as peptide biosynthesis and
268 translation (Figure 4E). To further characterize the RCG/DEGs, we used literature mining tool
269 BioLitMine and identified medical subject heading (MeSH) terms associated with RCG/DEGs
270 that were significantly enriched for several eye- and brain-relevant diseases, such as epilepsy,

271 eye abnormalities, and retinal and nerve degeneration (Figure 4F). Collectively, our data
272 showed that R-loops accumulated at both age up- and down-regulated genes, suggesting that
273 R-loops may contribute to gene expression regulation via multiple mechanisms. For example,
274 transcription can be blocked by direct collision of RNAP by pre-formed R-loops from previous
275 transcription rounds or alternatively, can be inhibited by an intrinsic R-loop formation in the wake
276 of ongoing RNAP. However, increased R-loop levels in age up-regulated genes may be simply
277 a result of increased expression of these genes. Importantly, given that R-loops accumulated at
278 most of the age down-regulated genes, which are enriched for long genes with neuronal
279 function, it suggests that R-loops may contribute to regulation of biological pathways relevant for
280 eye-specific functions.

281 **2.5 Top3β depletion in *Drosophila* PR neurons leads to increased R-loop levels and**
282 **decreased visual function**

283 The neuronal transcriptome is enriched for long and highly expressed genes, that undergo high
284 level of torsional stress during transcription (King et al., 2013; Liu & Wang, 1987). To solve DNA
285 and RNA topological problems, cells use conserved topoisomerase enzymes that play a critical
286 role in a wide range of fundamental metabolic processes in the genome (Pommier et al., 2016;
287 Wang, 2002). One of the enzymes is Top3β, a highly conserved, dual-activity topoisomerase in
288 animals that can change the topology of both DNA and RNA (Xu et al., 2013) and unwind
289 negatively supercoiled DNA that forms during transcription, an activity that prevents formation of
290 R-loops (Chedin & Benham, 2020). Loss of Top3β is associated with increased R-loop levels in
291 mammalian cells (Yang et al., 2014) and has been shown to reduce lifespan in mice (Kwan &
292 Wang, 2001). In addition, mutations in Top3β are linked to neurological disorders, thus
293 highlighting the critical role of Top3β in neuronal function (Joo et al., 2020). Interestingly, our
294 recent proteomic study of the aging *Drosophila* eye (Hall et al., 2021) revealed a 20% decrease
295 in Top3β protein levels (Figure 5A, Figure S5A), suggesting that the aging eye might be

296 sensitive to the loss of Top3β activity. Thus, we hypothesized that decreased Top3β levels
297 could contribute to changes in R-loop homeostasis and neuronal function in aging PRs. To test
298 this, we first depleted *Top3β* with ubiquitous RNAi in larvae (*tubP-Gal4>UAS-RNAi*) and
299 measured bulk R-loop levels. Using DNA slot blot and RNA-DNA-specific antibody S9.6, we
300 detected a 10% increase in R-loop levels in Top3β-depleted samples as compared to a control
301 expressing non-specific RNAi (Figure 5B-C). Pre-treatment of DNA samples with RNase H1 led
302 to a complete loss of the signal (Figure 5B-right), thus showing the specificity of the signal for
303 RNA-DNA hybrids. In addition, qPCR analysis of Top3β transcript levels showed approximately
304 80% reduction in Top3β-depleted samples as compared to a control, thus validating the
305 efficiency of the knockdown (Figure S5B). Taken together, these data show that Top3β in
306 *Drosophila* has a conserved role in maintenance of R-loop homeostasis.

307 Since loss of Top3β in *Drosophila* and mice leads to several neuronal phenotypes, such as
308 disruption of synapse formation and behavioral impairments, we were next interested to see if
309 depletion of Top3β specifically in PR neurons had any impact on visual function. Like most flying
310 insects, *Drosophila* move towards light, thus exhibiting positive phototaxis (Choe & Clandinin,
311 2005). Importantly, we and others showed that positive phototaxis declines with age in flies
312 (Carbone et al., 2016; Hall et al., 2017). To assess changes in visual behavior upon loss of
313 Top3β, we depleted Top3β transcripts specifically in photoreceptors using *Rh1-Gal4>UAS-RNAi*
314 and performed phototaxis assays at days 10 and 30 post-eclosion. As expected, there was
315 approximately 15% decrease in positive phototaxis in the control flies between day 10 and day
316 30 (Figure 5D-Supplemental file 2). Notably, while flies with PR-specific depletion of Top3β
317 showed no significant difference in the phototactic response at day 10, they showed
318 approximately 60% decrease in visual behavior at day 30 as compared to a control (Wilcoxon
319 test, p-value<0.47, and <0.015, respectively). Importantly, this decrease in visual behavior was
320 not due to the loss of PR neurons, as optical neutralization showed no retinal degeneration in

321 *Rh1-Gal4>UAS-RNAi* flies at day 30 post-eclosion (Figure 5E). Thus, our data show that Top3β
322 is required for maintenance of proper visual function in aging *Drosophila* photoreceptor neurons.

323 **2.6 Top3β regulates expression of a subset of long genes associated with neuronal**
324 **function in photoreceptors**

325 Given the role of Top3β in the resolution of torsional stress during transcription, we next
326 hypothesized that Top3β might be required to regulate the expression of genes with neuronal
327 function, which tend to be long and highly expresses (Zylka et al., 2015). To test this hypothesis,
328 we analyzed the transcriptome of PR neurons depleted for Top3β in *Rh1-Gal4>UAS-RNAi;*
329 *UAS-GFP*^{KASH} flies at day 30 using our NIE protocol. Differential expression analysis using
330 DESeq2 between Top3β-RNAi and control, revealed that expression of approximately 1% of
331 genes was regulated by Top3β (66 out 6500, FDR<0.05) (Figure 6A). Additionally, quantitative
332 analysis of gene length based on whether a gene was differentially expressed in Top3β
333 depleted PRs revealed, that genes with decreased expression were highly and significantly
334 enriched for long genes relative to genes that either increased or did not change expression
335 (Figure 6B). These data thus suggest that transcriptional regulation of long genes in the eye is
336 particularly sensitive to decreased Top3β levels. Gene Ontology (GO) enrichment analysis of all
337 Top3β-dependent genes revealed that genes with decreased expression were highly enriched
338 for genes with neuronal functions as shown by the gene concept network analysis (Cnetplot)
339 (Figure 6C). These genes included *Tenascin major* (*Ten-m; FBgn0004449*) and *Tenascin*
340 *accessory* (*Ten-a; FBgn0267001*), which form a transmembrane heterodimer involved in
341 synapsis regulation, *Tripartite motif containing 9* (*Trim9; FBgn0051721)*, a E3 ubiquitin ligase
342 involved in neurogenesis, axon guidance, and eye development, and *knockout* (*ko;*
343 *FBgn0020294),* a storkhead-box protein involved in axon guidance. Importantly, GO term
344 analysis of up-regulated genes did not lead to any significant biological category enrichment.

345 Thus, our data show that in PR neurons, Top3β is required to maintain gene expression levels
346 of long genes that are involved in neuronal function.

347 Next, we asked whether the expression of Top3β-dependent genes was mis-regulated during in
348 aging PR neurons. To do this, we compared genes that were down-regulated either during
349 aging or upon depletion of Top3β. Venn diagram revealed that 30% of Top3β-dependent genes
350 were also down-regulated during aging ("shared genes"), with the overlap being statistically
351 significant (Figure 6D). Further, individual inspection of these shared genes revealed that
352 majority of them were long and showed similar changes in fold change expression during aging
353 and Top3β depletion (Figure S6A). Thus, our data show that during aging, several long genes
354 important for neuronal function decrease expression in a Top3β-dependent manner. Further,
355 age- and Top3β-shared genes were significantly longer than Top3β-dependent genes (Figure
356 6E), suggesting that expression of longer genes is particularly sensitive to loss of Top3β during
357 aging. However, gene length analysis of genes differentially expressed during aging in PRs
358 revealed that down-regulated genes were significantly longer than up-regulated genes (Figure
359 6F-left). In addition, gene length analysis of our previously published RNA-seq data from aging
360 eyes of Rh1>GFP^{KASH} flies (Stegeman et al., 2018) revealed a similar trend (Figure 6F-right)
361 indicating that expression of the long genes in the aging retina is particularly sensitive to
362 dysregulation of molecular mechanisms that include Top3β.

363 Collectively, our data showed that Top3β is required to maintain expression of a specific subset
364 of genes with neuronal function that tend to be very long and thus are most likely sensitive to
365 loss of topoisomerase activity due to high levels of torsional stress. This suggests that during
366 aging, proper levels of Top3β are required to maintain R-loop homeostasis and expression of
367 genes important for visual function.

368 **2.7 Overexpression of Top3β or RNaseH1 enhances visual function during aging**

369 To further validate the role of topoisomerase activity and maintenance of R-loop homeostasis in
370 visual function during aging, we over-expressed either Top3β or human, nuclear localized,
371 RNASEH1 in *Drosophila* eyes under the control of longGMR-GAL4 driver, which induces high
372 expression in PRs and assessed visual behavior using phototaxis in 10-, 20-, and 30-day old
373 flies. Importantly, we validated that RNASEH1 is expressed using qPCR and showed that bulk
374 R-loop levels are decreased upon expression of RNASEH1 relative to a no driver control (Figure
375 S6B-C-D). In addition, we over-expressed Top3β under control of longGMR in a Top3β null
376 background (Top3β$^{-/-}$;longGMR>Top3β). Our data showed that at day 10, over-expression of
377 Top3β in the eyes of Top3β null flies resulted in similar light response as that of control flies
378 (Rh1>siControl, see Figure 5D) or longGMR>siControl flies (Stegeman et al., 2018) (Figure 6G-
379 Supplemental file 2). Furthermore, Top3β-/-; longGMR>Top3β flies showed an age-associated
380 decrease in positive light response which is consistent with control Rh1>siControl flies (Figure
381 6G-grey). Importantly, flies with Top3β over-expression (Top3β$^{+/+}$; longGMR>Top3β) showed an
382 enhanced positive light response at either day 10 or day 20 (Figure 6G-light blue), corroborating
383 that proper levels of Top3β contribute to visual response in flies. Moreover, over-expression of
384 RNase H1 in *Drosophila* eyes (Top3β$^{+/+}$; longGMR>RNaseH1) showed enhanced visual
385 response in 10- and 20-day old flies as compared to control flies, similar to that of flies with
386 Top3β over-expression (Figure 6G). These data suggest that Top3β function and R-loop
387 resolution by RNase H1 contribute to proper visual function in *Drosophila*. Notably, qPCR
388 analysis performed in flies with RNase H1 over-expression showed no significant difference in
389 Top3β transcript level as compared to that in wild type flies (Figure S6E – purple vs blue)
390 suggesting that the enhanced visual response in these flies is a result of increased R-loop
391 removal. However, all tested genotypes showed decreased positive phototaxis at 30 days post-
392 eclosion. Since optical microscopy imaging of the eyes did not show any changes in the eye
393 morphology in 30-day old flies (Figure S6F), these data imply that additional aging mechanisms

394 contribute to regulation of visual function in the eye, possibly including R-loops accumulated as
395 a result of aberrant expression of additional R-loop metabolism associated factors.

396 **3 DISCUSSION**

397 While R-loops were previously considered to be mere byproducts of transcription, it has been
398 demonstrated that R-loops play a significant physiological role in cellular biology of multiple
399 organisms, including humans. Notably, there is a growing body of evidence that links R-loop
400 accumulation to transcriptional imbalance and genomic instability, two main hallmarks of aging
401 (López-Otín et al., 2013). Furthermore, dysregulation of R-loop homeostasis has been linked to
402 human pathologies, including neurodegeneration (Groh & Gromak, 2014). Since age is the main
403 risk factor for many neurodegenerative diseases, our current study focused on characterizing
404 the changes in R-loop landscape induced during aging and evaluating the impact of R-loops on
405 the gene expression, specifically in *Drosophila* photoreceptor neurons.

406 Characterization of global R-loop levels in aging PRs showed an increase in R-loops by middle
407 age, with an additional significant increase late in aging. To our knowledge, this is the first
408 published report demonstrating changes in R-loop levels in a specific tissue during aging. To
409 further evaluate the R-loop distribution genome-wide, we modified a recently published R-loop
410 mapping strategy, called MapR, coupled with high-throughput sequencing that can be useful
411 when material is limiting. In addition, given that this method involves incubation of isolated
412 nuclei/cells with a recombinant mutant form of RNase H1 tethered with MNase and therefore
413 does not require modification of the organismal genome, it is well-suited for studies in whole
414 animals. Using this approach, our data demonstrated that R-loops covered approximately 10%
415 of the *Drosophila* PR genome, which is similar to the reported genomic distribution of R-loops in
416 other organisms (Sanz et al., 2016; Wahba et al., 2016). Consistent with previous reports, R-
417 loops were associated with known genomic hot-spots such as gene termini and specific genic
418 features such as high GC content, gene length and expression level. The aging transcriptomes

419 of multiple organisms and cell types show a positive correlation between transcriptional
420 downregulation and specific genic features, such as gene length and GC content (Stoeger et al.,
421 2019) and R-loops are known to play a key physiological role in transcription regulation due to
422 their presence at promoters and terminators, where they regulate transcription initiation and
423 termination, respectively (Niehrs & Luke, 2020). Thus, R-loop accumulation over these genomic
424 regions may be a conserved mechanism that contributes to gene expression regulation in
425 multiple cell types, including neurons.

426 Further, we observed a significant increase in R-loop signal over gene bodies and importantly,
427 age-associated broadening of R-loop peak signal, suggesting that aging neurons accumulate R-
428 loops at higher rate or R-loops are more persistent and potentially extend with age.
429 Transcriptome of neurons is biased for longer transcript relative to non-neuronal cell types
430 (Zylka et al., 2015). Notably, long genes accumulate high topological stress during transcription
431 and loss of topoisomerase activity has been shown to preferentially inhibit expression of (López-
432 Otín et al. 2013) long genes (King et al., 2013). Since age-associated R-loop gains were
433 particularly localized at long and highly expressed genes, we sought to further explore the
434 impact of decreased topoisomerase activity on the maintenance of photoreceptor neuron
435 homeostasis. DNA/RNA topoisomerase Top3β dysfunction is associated with increased R-loop
436 levels in mammalian cells and mutations in Top3β are linked to neurological disorders, thus
437 highlighting the critical role of Top3β in neuronal function (Joo et al., 2020). Importantly, Top3β
438 protein levels decrease in aging *Drosophila* eyes (Hall et al., 2021). Here, we demonstrated that
439 normal Top3β levels were required for maintenance of neuronal function, as shown by an age-
440 associated decrease in visual behavior upon photoreceptor-specific downregulation of Top3β. In
441 addition, depletion of Top3β in PRs lead to decreased expression of a subset of long genes with
442 neuronal function, some of which also gained R-loop levels with age. Moreover, Top3β or
443 RNase H1 over-expression in the eyes enhanced positive light response in flies and mitigated

444 age-dependent loss of visual function. Collectively, our data suggest that Top3β may function in
445 regulation of gene expression and maintenance of R-loop homeostasis in a subset of long
446 genes required for neuronal function in aging photoreceptors. Thus, imbalance in R-loop
447 homeostasis during aging could make postmitotic neurons particularly susceptible to
448 dysregulation of gene expression and loss of function leading to increased risk of age-related
449 neurodegeneration.

450 Aging is accompanied by elevated incidence of ocular diseases such as age-related macular
451 degeneration and glaucoma, which exhibit characteristics of neurodegenerative diseases
452 including loss of function and irreversible neuronal cell loss. How does aging impact
453 development and progression of age-associated chronic diseases is one of the key questions in
454 the biology of aging. Our current studies demonstrate a novel finding that *Drosophila*
455 photoreceptor neurons progressively accumulate R-loops during aging, mostly at long and
456 highly expressed genes. Importantly, integration of our transcriptomic and R-loop mapping data
457 shows that majority of genes that decrease expression in aging PRs accumulate R-loops, thus
458 suggesting that R-loops could be involved in cell physiology of aging neurons via inhibition of
459 gene expression. Moreover, persistent formation of R-loops often leads to increased DNA
460 damage, which is associated both with aging and neurodegeneration. Given that mutations in
461 number of proteins involved in R-loop biology are implicated in neurodegenerative disease, our
462 studies suggest that both aging and neurodegeneration may be sensitive to dysfunction in
463 similar pathways.

464 **4 EXPERIMENTAL PROCEDURES**

465 See Supporting Information

466 **ACKNOWLEDGMENTS**

467 Fly stocks from the Bloomington Drosophila Stock Center and information from FlyBase were
468 used in this study.

469 **CONFLICT OF INTEREST**

470 The authors declare that they have no competing interests.

471 **AUTHOR CONTRIBUTIONS**

472 J.J-L. performed all the NGS experiments, bioinformatics analysis and figure generation. N.A.L.
473 and V.M.W. assisted with data analysis. S. E. performed the phototaxis assay. A.N.E. and H.H.
474 performed the slot blots and Western blots. J.J-L. and H.H. wrote the manuscript with input from
475 other authors. H.H. supervised the project and conceived the study.

476 **ORCID**

477 Juan Jauregui-Lozano https://orcid.org/0000-0001-6633-9152
478 Spencer E Escobedo https://orcid.org/0000-0002-9026-9104
479 Alyssa N Easton https://orcid.org/0000-0002-0972-3630
480 Nadia A Lanman https://orcid.org/0000-0002-1819-7070
481 Vikki M. Weake https://orcid.org/0000-0002-5933-9952
482 Hana Hall https://orcid.org/0000-0002-7544-4437
483

484 **DATA AVAILABILITY**

485 RNA-seq expression data and MapR mapping data are accessible through Gene Expression
486 Omnibus repository under series accession numbers GSE174488, GSE174491 and
487 GSE174515, respectively. The following link has been created to allow reviewers to access
488 these records while they remain in private status.
489

490 **HOW TO CITE THIS ARTICLE**

491 Jauregui-Lozano J, Escobedo SE, Easton AN, Lanman NA, Weake VM, Hall H. Proper control
492 of R-loop homeostasis is required for maintenance of gene expression and neuronal function
493 during aging

494 **REFERENCES**

495 Aguilera, A., & García-Muse, T. (2012). R Loops: From Transcription Byproducts to Threats to
496 Genome Stability. *Molecular Cell*, *46*(2), 115–124.
497 https://doi.org/10.1016/j.molcel.2012.04.009

498 Alecki, C., Chiwara, V., Sanz, L. A., Grau, D., Arias Pérez, O., Boulier, E. L., Armache, K.-J.,
499 Chédin, F., & Francis, N. J. (2020). RNA-DNA strand exchange by the Drosophila
500 Polycomb complex PRC2. *Nature Communications*, *11*(1), 1781.
501 https://doi.org/10.1038/s41467-020-15609-x

502 Allison, D. F., & Wang, G. G. (2019). R-loops: Formation, function, and relevance to cell stress.
503 *Cell Stress*, *3*(2), 38–46. https://doi.org/10.15698/cst2019.02.175

504 Belotserkovskii, B. P., Tornaletti, S., D'Souza, A. D., & Hanawalt, P. C. (2018). R-loop
505 generation during transcription: Formation, processing and cellular outcomes. *DNA*
506 *Repair*, *71*, 69–81. https://doi.org/10.1016/j.dnarep.2018.08.009

507 Bentin, T., Cherny, D., Larsen, H. J., & Nielsen, P. E. (2005). Transcription arrest caused by
508 long nascent RNA chains. *Biochimica et Biophysica Acta (BBA) - Gene Structure and*
509 *Expression*, *1727*(2), 97–105. https://doi.org/10.1016/j.bbaexp.2004.12.006

510 Bonnel, S., Mohand-Said, S., & Sahel, J.-A. (2003). The aging of the retina. *Experimental*
511 *Gerontology*, *38*(8), 825–831. https://doi.org/10.1016/S0531-5565(03)00093-7

512 Boque-Sastre, R., Soler, M., Oliveira-Mateos, C., Portela, A., Moutinho, C., Sayols, S.,
513 Villanueva, A., Esteller, M., & Guil, S. (2015). Head-to-head antisense transcription and
514 R-loop formation promotes transcriptional activation. *Proceedings of the National*
515 *Academy of Sciences*, *112*(18), 5785–5790.

516 Carbone, M. A., Yamamoto, A., Huang, W., Lyman, R. A., Meadors, T. B., Yamamoto, R.,
517 Anholt, R. R. H., & Mackay, T. F. C. (2016). Genetic architecture of natural variation in

518 visual senescence in Drosophila. *Proceedings of the National Academy of Sciences*,
519 *113*(43), E6620–E6629. https://doi.org/10.1073/pnas.1613833113
520 Chedin, F., & Benham, C. J. (2020). Emerging roles for R-loop structures in the management of
521 topological stress. *The Journal of Biological Chemistry*, *295*(14), 4684–4695.
522 https://doi.org/10.1074/jbc.REV119.006364
523 Choe, K., & Clandinin, T. R. (2005). Thinking about Visual Behavior; Learning about
524 Photoreceptor Function. In *Current Topics in Developmental Biology* (Vol. 69, pp. 187–
525 213). Academic Press. https://doi.org/10.1016/S0070-2153(05)69007-2
526 Groh, M., & Gromak, N. (2014). Out of Balance: R-loops in Human Disease. *PLOS Genetics*,
527 *10*(9), e1004630. https://doi.org/10.1371/journal.pgen.1004630
528 Grotewiel, M. S., Martin, I., Bhandari, P., & Cook-Wiens, E. (2005). Functional senescence in
529 Drosophila melanogaster. *Ageing Research Reviews*, *4*(3), 372–397.
530 https://doi.org/10.1016/j.arr.2005.04.001
531 Hall, H., Cooper, B. R., Qi, G., Wijeratne, A. B., Mosley, A. L., & Weake, V. M. (2021).
532 Quantitative Proteomic and Metabolomic Profiling Reveals Altered Mitochondrial
533 Metabolism and Folate Biosynthesis Pathways in the Aging Drosophila Eye. *Molecular &*
534 *Cellular Proteomics : MCP*, *20*, 100127. https://doi.org/10.1016/j.mcpro.2021.100127
535 Hall, H., Medina, P., Cooper, D. A., Escobedo, S. E., Rounds, J., Brennan, K. J., Vincent, C.,
536 Miura, P., Doerge, R., & Weake, V. M. (2017). Transcriptome profiling of aging
537 Drosophila photoreceptors reveals gene expression trends that correlate with visual
538 senescence. *BMC Genomics*, *18*(1), 894. https://doi.org/10.1186/s12864-017-4304-3
539 Hu, Y., Chung, V., Comjean, A., Rodiger, J., Nipun, F., Perrimon, N., & Mohr, S. E. (2020).
540 BioLitMine: Advanced Mining of Biomedical and Biological Literature About Human
541 Genes and Genes from Major Model Organisms. *G3: Genes|Genomes|Genetics*, *10*(12),
542 4531–4539. https://doi.org/10.1534/g3.120.401775

543 Jackson, G. R., Owsley, C., & Curcio, C. A. (2002). Photoreceptor degeneration and dysfunction
544 in aging and age-related maculopathy. *Ageing Research Reviews*, *1*(3), 381–396.
545 https://doi.org/10.1016/S1568-1637(02)00007-7
546 Jauregui-Lozano, J., Bakhle, K., & Weake, V. M. (2021). In vivo tissue-specific chromatin
547 profiling in Drosophila melanogaster using GFP-tagged nuclei. *Genetics*, *218*(3).
548 https://doi.org/10.1093/genetics/iyab079
549 Joo, Y., Xue, Y., Wang, Y., McDevitt, R. A., Sah, N., Bossi, S., Su, S., Lee, S. K., Peng, W., Xie,
550 A., Zhang, Y., Ding, Y., Ku, W. L., Ghosh, S., Fishbein, K., Shen, W., Spencer, R.,
551 Becker, K., Zhao, K., … Wang, W. (2020). Topoisomerase 3β knockout mice show
552 transcriptional and behavioural impairments associated with neurogenesis and synaptic
553 plasticity. *Nature Communications*, *11*(1), 3143. https://doi.org/10.1038/s41467-020-
554 16884-4
555 King, I. F., Yandava, C. N., Mabb, A. M., Hsiao, J. S., Huang, H.-S., Pearson, B. L., Calabrese,
556 J. M., Starmer, J., Parker, J. S., Magnuson, T., Chamberlain, S. J., Philpot, B. D., &
557 Zylka, M. J. (2013). Topoisomerases facilitate transcription of long genes linked to
558 autism. *Nature*, *501*, 58. https://doi.org/10.1038/nature12504
559 Kwan, K. Y., & Wang, J. C. (2001). Mice lacking DNA topoisomerase IIIβ develop to maturity but
560 show a reduced mean lifespan. *Proceedings of the National Academy of Sciences*,
561 *98*(10), 5717–5721. https://doi.org/10.1073/pnas.101132498
562 Liu, L. F., & Wang, J. C. (1987). Supercoiling of the DNA template during transcription.
563 *Proceedings of the National Academy of Sciences*, *84*(20), 7024–7027.
564 Lopes, I., Altab, G., Raina, P., & de Magalhães, J. P. (2021). Gene Size Matters: An Analysis of
565 Gene Length in the Human Genome. *Frontiers in Genetics*, *12*, 30.
566 https://doi.org/10.3389/fgene.2021.559998
567 López-Otín, C., Blasco, M. A., Partridge, L., Serrano, M., & Kroemer, G. (2013). The Hallmarks
568 of Aging. *Cell*, *153*(6), 1194–1217. https://doi.org/10.1016/j.cell.2013.05.039

569 Mackay, R. P., Xu, Q., & Weinberger, P. M. (2020). R-Loop Physiology and Pathology: A Brief
570 Review. *DNA and Cell Biology*, *39*(11), 1914–1925.
571 https://doi.org/10.1089/dna.2020.5906
572 McKinnon, P. J. (2016). Topoisomerases and the regulation of neural function. *Nature Reviews.*
573 *Neuroscience*, *17*(11), 673–679. https://doi.org/10.1038/nrn.2016.101
574 Niehrs, C., & Luke, B. (2020). Regulatory R-loops as facilitators of gene expression and
575 genome stability. *Nature Reviews Molecular Cell Biology*, 1–12.
576 https://doi.org/10.1038/s41580-019-0206-3
577 Parapuram, S. K., Cojocaru, R. I., Chang, J. R., Khanna, R., Brooks, M., Othman, M., Zareparsi,
578 S., Khan, N. W., Gotoh, N., Cogliati, T., & Swaroop, A. (2010). Distinct signature of
579 altered homeostasis in aging rod photoreceptors: Implications for retinal diseases. *PloS*
580 *One*, *5*(11), e13885. https://doi.org/10.1371/journal.pone.0013885
581 Pommier, Y., Sun, Y., Huang, S. N., & Nitiss, J. L. (2016). Roles of eukaryotic topoisomerases
582 in transcription, replication and genomic stability. *Nature Reviews Molecular Cell*
583 *Biology*, *17*, 703. https://doi.org/10.1038/nrm.2016.111
584 Rauser, C. L., Abdel-Aal, Y., Shieh, J. A., Suen, C. W., Mueller, L. D., & Rose, M. R. (2005).
585 Lifelong heterogeneity in fecundity is insufficient to explain late-life fecundity plateaus in
586 Drosophila melanogaster. *Experimental Gerontology*, *40*(8), 660–670.
587 https://doi.org/10.1016/j.exger.2005.06.006
588 Sanz, L. A., Hartono, S. R., Lim, Y. W., Steyaert, S., Rajpurkar, A., Ginno, P. A., Xu, X., &
589 Chédin, F. (2016). Prevalent, Dynamic, and Conserved R-Loop Structures Associate
590 with Specific Epigenomic Signatures in Mammals. *Molecular Cell*, *63*(1), 167–178.
591 https://doi.org/10.1016/j.molcel.2016.05.032
592 Simon, A. F., Liang, D. T., & Krantz, D. E. (2006). Differential decline in behavioral performance
593 of Drosophila melanogaster with age. *Mechanisms of Ageing and Development*, *127*(7),
594 647–651. https://doi.org/10.1016/j.mad.2006.02.006

595 Skourti-Stathaki, K., Kamieniarz-Gdula, K., & Proudfoot, N. J. (2014). R-loops induce repressive
596 chromatin marks over mammalian gene terminators. *Nature*, *516*(7531), 436–439.
597 https://doi.org/10.1038/nature13787
598 Skourti-Stathaki, K., Proudfoot, N. J., & Gromak, N. (2011). Human Senataxin Resolves
599 RNA/DNA Hybrids Formed at Transcriptional Pause Sites to Promote Xrn2-Dependent
600 Termination. *Molecular Cell*, *42*(6), 794–805.
601 https://doi.org/10.1016/j.molcel.2011.04.026
602 Stegeman, R., Hall, H., Escobedo, S. E., Chang, H. C., & Weake, V. M. (2018). Proper splicing
603 contributes to visual function in the aging Drosophila eye. *Aging Cell*, *17*(5), e12817.
604 https://doi.org/10.1111/acel.12817
605 Stoeger, T., Grant, R. A., McQuattie-Pimentel, A. C., Anekalla, K., Liu, S. S., Tejedor-Navarro,
606 H., Singer, B. D., Abdala-Valencia, H., Schwake, M., Tetreault, M.-P., Perlman, H.,
607 Balch, W. E., Chandel, N., Ridge, K., Sznajder, J. I., Morimoto, R. I., Misharin, A. V.,
608 Budinger, G. R. S., & Amaral, L. A. N. (2019). Aging is associated with a systemic
609 length-driven transcriptome imbalance. *BioRxiv*, 691154. https://doi.org/10.1101/691154
610 Tous, C., & Aguilera, A. (2007). Impairment of transcription elongation by R-loops in vitro.
611 *Biochemical and Biophysical Research Communications*, *360*(2), 428–432.
612 https://doi.org/10.1016/j.bbrc.2007.06.098
613 Wahba, L., Costantino, L., Tan, F. J., Zimmer, A., & Koshland, D. (2016). S1-DRIP-seq
614 identifies high expression and polyA tracts as major contributors to R-loop formation.
615 *Genes & Development*, *30*(11), 1327–1338. https://doi.org/10.1101/gad.280834.116
616 Wang, J. C. (2002). Cellular roles of DNA topoisomerases: A molecular perspective. *Nature*
617 *Reviews Molecular Cell Biology*, *3*(6), 430–440. https://doi.org/10.1038/nrm831
618 Xu, D., Shen, W., Guo, R., Xue, Y., Peng, W., Sima, J., Yang, J., Sharov, A., Srikantan, S.,
619 Yang, J., Fox, D., Qian, Y., Martindale, J. L., Piao, Y., Machamer, J., Joshi, S. R.,
620 Mohanty, S., Shaw, A. C., Lloyd, T. E., … Wang, W. (2013). Top3β is an RNA

621 topoisomerase that works with Fragile X syndrome protein to promote synapse
622 formation. *Nature Neuroscience*, *16*(9), 1238–1247. https://doi.org/10.1038/nn.3479
623 Yan, Q., & Sarma, K. (2020). MapR: A Method for Identifying Native R-Loops Genome Wide.
624 *Current Protocols in Molecular Biology*, *130*(1), e113. https://doi.org/10.1002/cpmb.113
625 Yang, Y., McBride, K. M., Hensley, S., Lu, Y., Chedin, F., & Bedford, M. T. (2014). Arginine
626 Methylation Facilitates the Recruitment of TOP3B to Chromatin to Prevent R Loop
627 Accumulation. *Molecular Cell*, *53*(3), 484–497.
628 https://doi.org/10.1016/j.molcel.2014.01.011
629 Zhang, T., Wallis, M., Petrovic, V., Challis, J., Kalitsis, P., & Hudson, D. F. (2020). Loss of
630 TOP3B leads to increased R-loop formation and genome instability. *Open Biology*,
631 *9*(12), 190222. https://doi.org/10.1098/rsob.190222
632 Zylka, M. J., Simon, J. M., & Philpot, B. D. (2015). Gene Length Matters in Neurons. *Neuron*,
633 *86*(2), 353–355. https://doi.org/10.1016/j.neuron.2015.03.059
634

635 **FIGURE LEGENDS**

636 **Figure 1.** Aging photoreceptor neurons show increased global R-loop levels that correlate with
637 loss of function and precede age-associated retinal degeneration.

638 (a) Schematic of experimental outline to detect global levels of R-loops in aging photoreceptor
639 neurons. Top: diagram of the cellular localization of the GFP^{KASH} protein. Dark blue lines
640 represent each lipid layer within the nuclear membrane. Bottom: diagram of an ommatidium, a
641 structural subunit in the *Drosophila* compound eye. Each ommatidium is composed of 8
642 photoreceptor neurons, labeled R1 to R8. Outer photoreceptors (R1-R6) express the *ninaE*
643 (Rh1) gene.

644 (b) Slot blot analysis of R-loop levels from photoreceptor nuclei at day 10, 30 and 50 post-
645 eclosion treated with (right) or without (left) RNase H1. Slot blots were performed using RNA-
646 DNA hybrid-specific S9.6 antibody (top) and ssDNA for loading control (bottom).

647 (c) Quantification of S9.6 slot blot signal in aging PRs from (b). Values above 1 represent
648 increase signal relative to day 10. Mean +/- Standard Deviation (SD), (n=2).

649 **Figure 2**. Profiling genome-wide R-loop distribution in PR neurons reveals age-associated
650 changes.

651 (a) Schematic diagram of the R-loop mapping technique used in this study (MapR). Immuno-
652 enriched nuclei are incubated with ΔRNaseH1-MNase (ΔRH-MNase), where ΔRH binds to R-
653 loops. Ionic activation of MNase results in cleavage of surrounding DNA and subsequent R-loop
654 enriched DNA release, which is purified and used for sequencing library preparation.

655 (b) Genome browser inspection of MapR track data on integrated genomic viewer (IgV) for a
656 selected genomic region. Three independent biological replicates (R1-R3) from 10-day old flies'
657 samples not pre-treated with RNaseH1 are shown in black, and a sample from nuclei that were
658 pre-treated with RNaseH1 prior to MapR (see Methods) is shown in blue. Peaks obtained using
659 MACS2 for each sample are also shown as bars under each corresponding sample track.

660 (c) Metaplot of CPM-normalized MapR signal over gene bodies for samples that were pre-
661 treated with (blue) or without (black) RNase H1 prior to MapR (from b).

662 (d) Spearman correlation heatmap of Aging MapR read distribution over 1000-bp binned
663 genome. Scores between 0 and 1 shown in each box correspond to Spearman's rank score.

664 (e) Principal component analysis (PCA) of Aging MapR samples based on read distribution over
665 1000-bp binned genome.

666 **Figure 3.** Age-associated accumulation of R-loops over gene bodies correlates with high GC
667 content, gene length and transcript levels.

668 (a) Metaplot of CPM-normalized MapR signal over gene bodies for all genes across age-
669 timepoints. Signal is an average obtained from three independent biological replicates per age-
670 timepoint. TSS indicates Transcription Start Site and TTS indicates Transcription Termination
671 Site.

672 (b) Metaplot of CPM-normalized Aging MapR signal around peaks obtained using MACS2
673 during aging.

674 (c) Boxplot of genomic coverage of Aging MapR signal as defined by the total sum of peak width
675 obtained at each time point. Peaks that mapped to scaffold or non-defined chromosomes were
676 excluded from analysis. We used Wilcoxon Rank-Sum test to compare pair-wise differences in
677 the distribution of genomic coverage amongst ages, (n=3).

678 (d) Heatmap showing log2 ratios of Aging MapR signal around the TSS (top) or TTS (bottom),
679 comparing day 50 to day 10. Genes are ranked based on their fold change value and divided in
680 four groups (quartiles) based on their position on the heatmap.

681 (e) Boxplot analysis of GC content, gene length and expression levels for each group of genes
682 divided in four groups based on the Aging MapR fold changes around TSS (top) and TTS
683 (bottom). p-value is obtained using Wilcoxon test.

684 **Figure 4.** Accumulation of R-loops in long genes correlates with decreased transcript levels in
685 aging PRs.

686 (a) Volcano plot representing differentially expressed genes (DEGs) between day 50 and day
687 10. DEGs are obtained using DESeq2 (adjusted p-value < 0.05, |FC|>1.5).

688 (b) Venn diagram representing the overlap between R-loop containing genes (RCGs) and DEGs
689 from (a).

690 (c) Box plot analysis of gene length for differentially expressed genes, R-loop containing genes,
691 or RCG/DEGs from (b). p-value is obtained using Wilcoxon test.

692 (d) Hierarchically clustered heatmap of RNA-seq data for RCG/DEGs from (b). Normalized Z-
693 scores are calculated based on normalized counts obtained using DESeq2, and the heatmap is
694 divided into genes that were either up- or down-regulated with age.

695 (e) Dot plot of biological processes identified as significantly enriched in Gene Ontology (GO)
696 term analysis for genes that were either up- or down-regulated from (d).

697 (f) Scatter plot depicting an enrichment analysis of diseases associated with genes that were
698 down-regulated with age and contained at least one R-loop. Analysis performed using literature
699 mining tool BioLitMine (Hu et al., 2020). A lower score (x-axis) represents higher enrichment.

700 **Figure 5.** Loss of *Drosophila* Top3β leads to increased R-loop levels.

701 (a) Comparison of Top3β protein levels in aging eyes from Rh1>GFP^{KASH} flies, shown as
702 normalized protein abundance. Proteomic samples were prepared from 10- and 40-day old flies,
703 100 eyes/sample (n=4). Raw data taken from (Hall et al., 2021).

704 (b) Slot blot analysis of R-loop levels from 3rd instar larvae ubiquitously expressing siRNA
705 against mCherry (siControl) or against Top3β (siTop3β). Samples were treated with (right) or
706 without (left) RNase H1. Slot blots were performed using S9.6 antibody (top) and ssDNA for
707 loading control (bottom).

708 (c) Quantification of S9.6 slot blot from (b). S9.6 signal is normalized to ssDNA slot blot signal,
709 (n=3).

710 (d) Box plots showing the light preference indices (positive phototaxis) for Rh1>GFP^{KASH},
711 mCherry-RNAi (siControl) or Rh1>GFP^{KASH}, Top3β-RNAi (siTop3β) at day 10 and 30 (6
712 biological replicates for each time point or RNAi, 27 - 33 male flies/replicate; total number of flies
713 per fly strain=150-180). p value obtained using Wilcoxon test.

714 (e) Optic neutralization of siControl and siTop3β at day 10 and 30 post-eclosion from (d). Retinal
715 degeneration (RD) scores were obtained by blindly quantifying 5 biological replicates. Score of
716 0% means there was no observable loss of rhabdomere or ommatidia.

717 **Figure 6.** Top3β regulates expression of a subset of long genes associated with neuronal
718 function in photoreceptors.

719 (a) Volcano plot representing differentially expressed genes (DEGs) between siTop3β and
720 siControl-expressing photoreceptors at day 30 post eclosion. DEGs obtained using DESeq2
721 (adjusted p-value < 0.05, |FC|>1.5). Size of each point reflect the gene length of the whole gene
722 as defined as most upstream TSS and most downstream TTS.

723 (b) Box plots showing the gene length (as log_2-transformed bp) for genes identified as down-,
724 up- or not regulated using DESeq2 in siTop3β photoreceptors relative to siControl (adjusted p-
725 value < 0.05, |FC|>1.5). p-value obtained using Wilcoxon test.

726 (c) Gene concept network analysis (Cnetplot) of genes downregulated in siTop3β
727 photoreceptors relative to siControl. Gene length in kilobases is shown next to each gene.

728 (d) Venn diagram representing the overlap of genes that were down-regulated in either aging
729 (D50 vs D10) or upon loss of Top3β (siTop3β vs siControl). Overlap significance is denoted as a
730 “overlapping p-value”, obtained with a hypergeometric test. Odds ratio and Jaccard index are
731 measurements of similarity.

732 (e) Box plots showing the gene length (as log_2-transformed bp) for genes in the overlap
733 identified in (d) or genes that were regulated by Top3β but not during aging. p-value is obtained
734 using Wilcoxon test.

735 (f) Box plots showing the gene length (as log_{10}-transformed bp) for genes that were identified as
736 down- or up-regulated in either aging PRs (left) or eyes (right). Eye data was obtained from
737 (Stegeman et al., 2018).

738 (g) Box plots showing the light preference indices (positive phototaxis) for Top3β-/-;
739 longGMR>Top3β, Top3β-/-; longGMR>Top3β, and longGRM>RNaseH1 at day 10, 20, and 30
740 post-eclosion (6 biological replicates for sample; 29 - 31 male flies/experiment; total number of
741 flies ~180). p-value obtained using Wilcoxon test.

742 **Supplemental File 1.** Summary of uniquely mapped fragments for Aging MapR samples to
743 *Drosophila melanogaster* dm6 genome.

744 **Supplemental File 2.** Raw data obtained in phototaxis assay for Figure 5D and Figure 6G

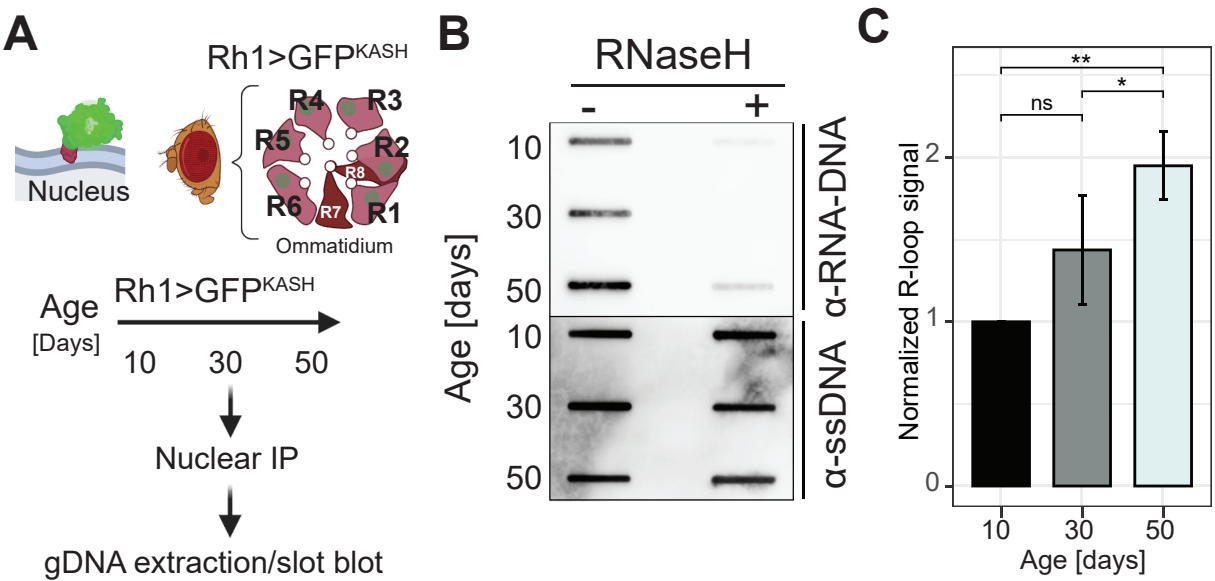
A
Rh1>GFP^KASH
Nucleus
R4
R3
R5
R2
R8
R6
R7
R1
Ommatidium
Age
[Days]
Rh1>GFP^KASH
10
30
50
Nuclear IP
gDNA extraction/slot blot
B
RNaseH
-
+
Age [days]
10
30
50
10
30
50
α-RNA-DNA
α-ssDNA
C
**
*
ns
Normalized R-loop signal
0
1
2
10
30
50
Age [days]

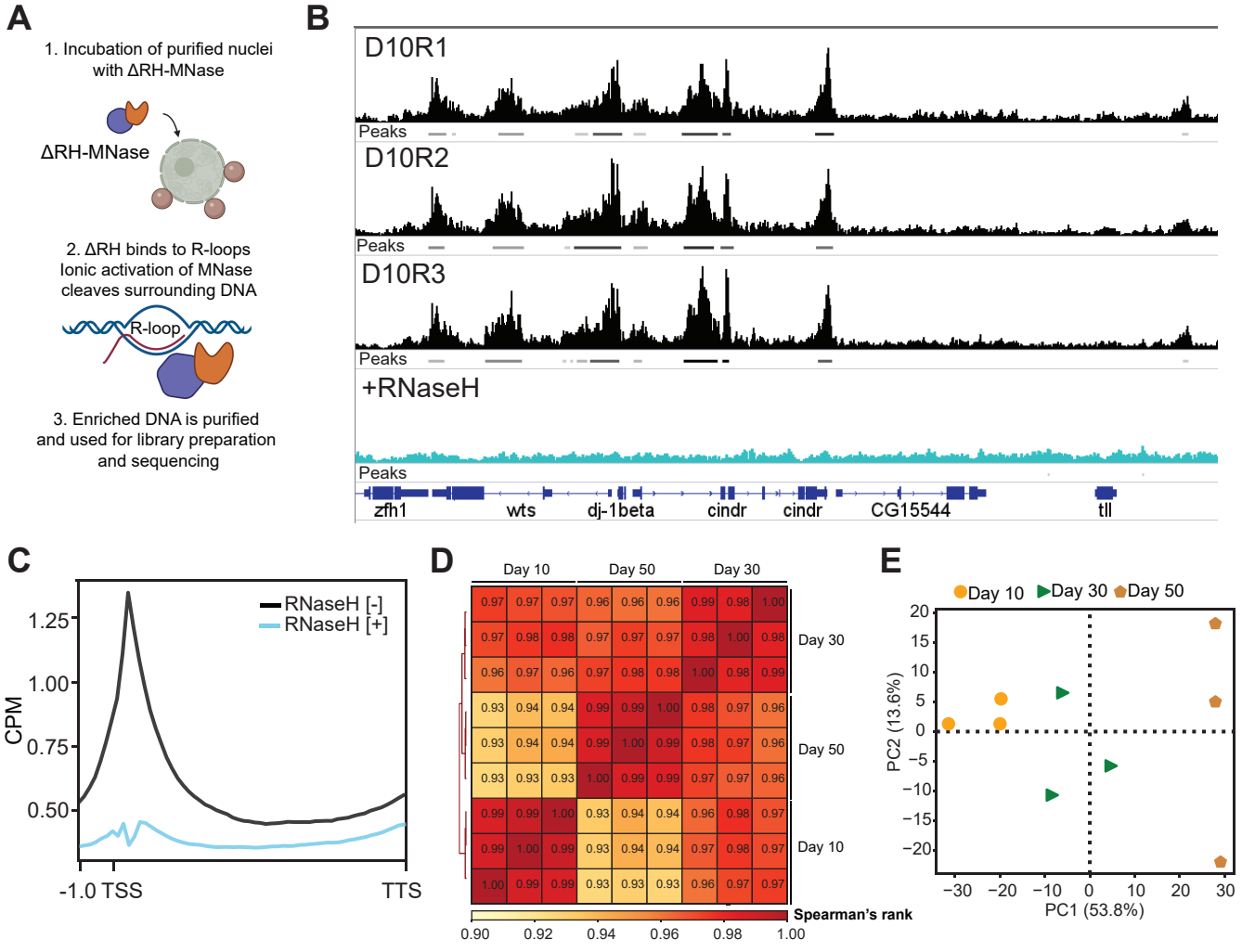
A
1. Incubation of purified nuclei with ΔRH-MNase
ΔRH-MNase
2. ΔRH binds to R-loops
Ionic activation of MNase cleaves surrounding DNA
R-loop
3. Enriched DNA is purified and used for library preparation and sequencing
B
D10R1
Peaks
D10R2
Peaks
D10R3
Peaks
+RNaseH
Peaks
zfh1
wts
dj-1beta
cindr
cindr
CG15544
tll
C
RNaseH [-]
RNaseH [+]
CPM
1.25
1.00
0.75
0.50
-1.0 TSS
TTS
D
Day 10
Day 50
Day 30
Day 30
Day 50
Day 10
Spearman's rank
0.90
0.92
0.94
0.96
0.98
1.00
E
Day 10
Day 30
Day 50
PC2 (13.6%)
PC1 (53.8%)

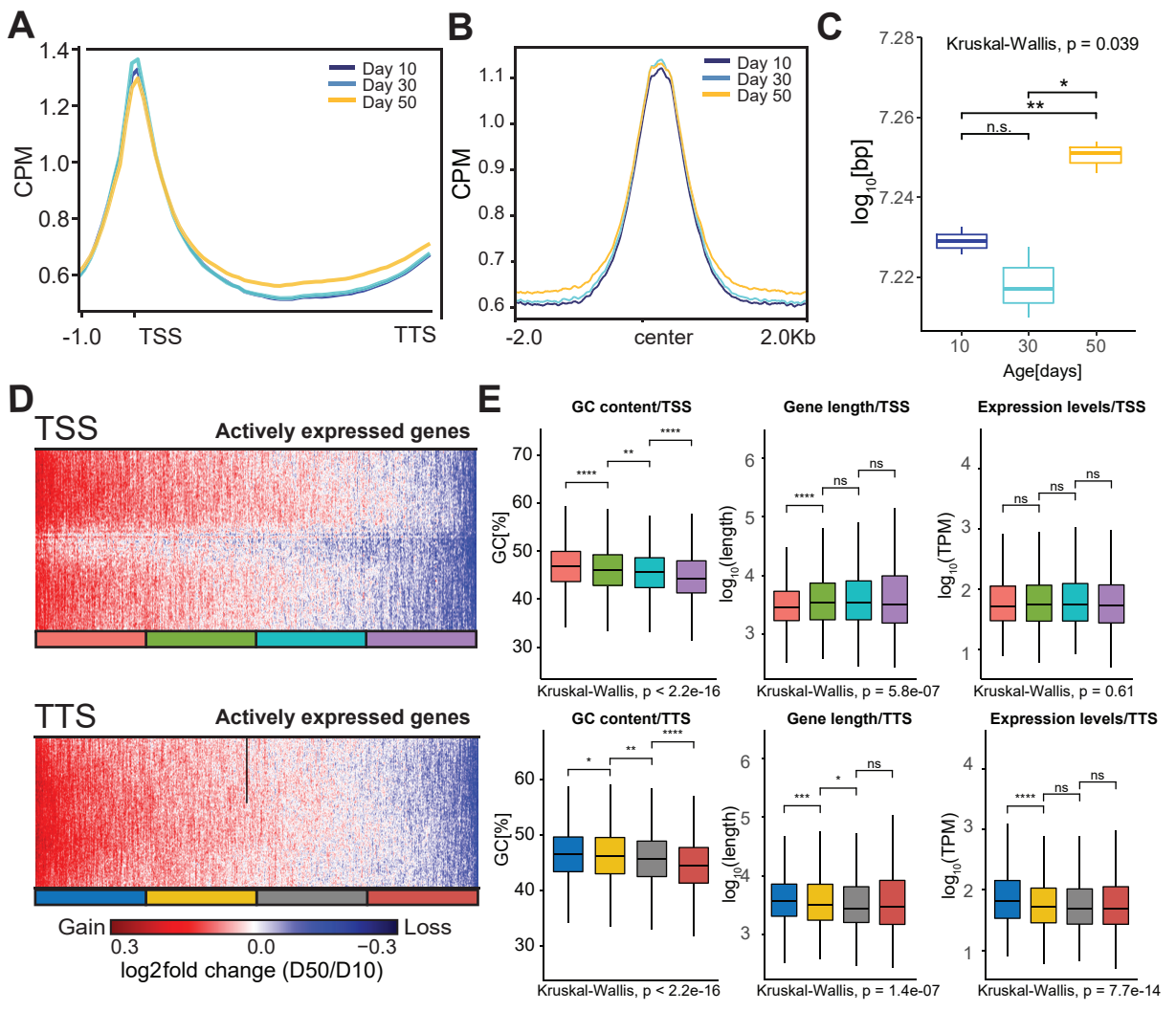
A
CPM
Day 10
Day 30
Day 50
-1.0
TSS
TTS
B
CPM
Day 10
Day 30
Day 50
-2.0
center
2.0Kb
C
Kruskal-Wallis, p = 0.039
log10[bp]
n.s.
**
*
Age[days]
D
TSS
Actively expressed genes
TTS
Actively expressed genes
Gain
Loss
0.3
0.0
−0.3
log2fold change (D50/D10)
E
GC content/TSS
Kruskal-Wallis, p < 2.2e-16
Gene length/TSS
Kruskal-Wallis, p = 5.8e-07
Expression levels/TSS
Kruskal-Wallis, p = 0.61
GC content/TTS
Kruskal-Wallis, p < 2.2e-16
Gene length/TTS
Kruskal-Wallis, p = 1.4e-07
Expression levels/TTS
Kruskal-Wallis, p = 7.7e-14
GC[%]
log10(length)
log10(TPM)
ns

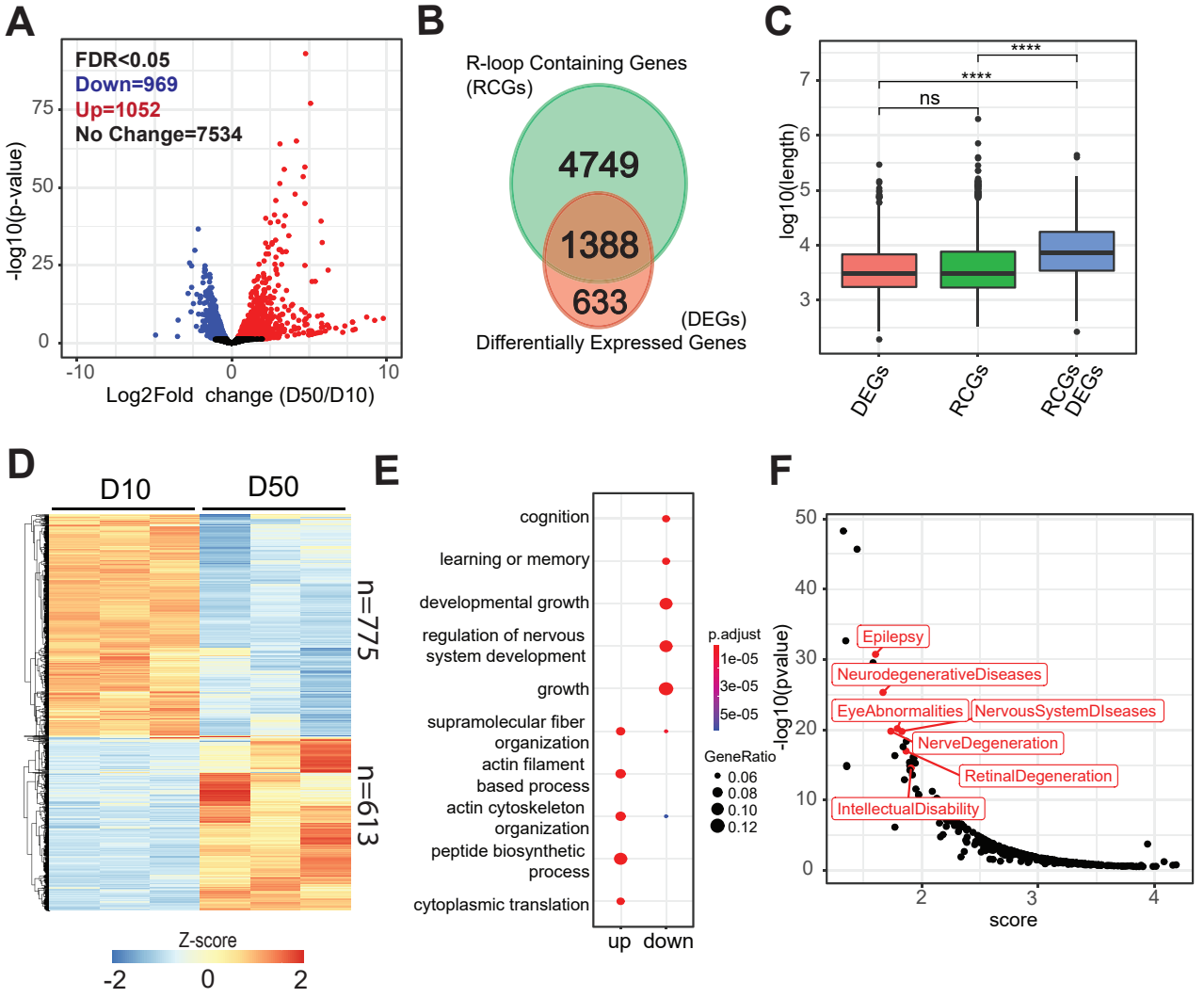
A
FDR<0.05
Down=969
Up=1052
No Change=7534
-log10(p-value)
Log2Fold change (D50/D10)
B
R-loop Containing Genes
(RCGs)
4749
1388
633
(DEGs)
Differentially Expressed Genes
C
log10(length)
ns
****
****
DEGs
RCGs
RCGs DEGs
D
D10
D50
n=775
n=613
Z-score
E
cognition
learning or memory
developmental growth
regulation of nervous system development
growth
supramolecular fiber organization
actin filament based process
actin cytoskeleton organization
peptide biosynthetic process
cytoplasmic translation
up
down
p.adjust
GeneRatio
F
-log10(pvalue)
score
Epilepsy
NeurodegenerativeDiseases
EyeAbnormalities
NervousSystemDIseases
NerveDegeneration
RetinalDegeneration
IntellectualDisability

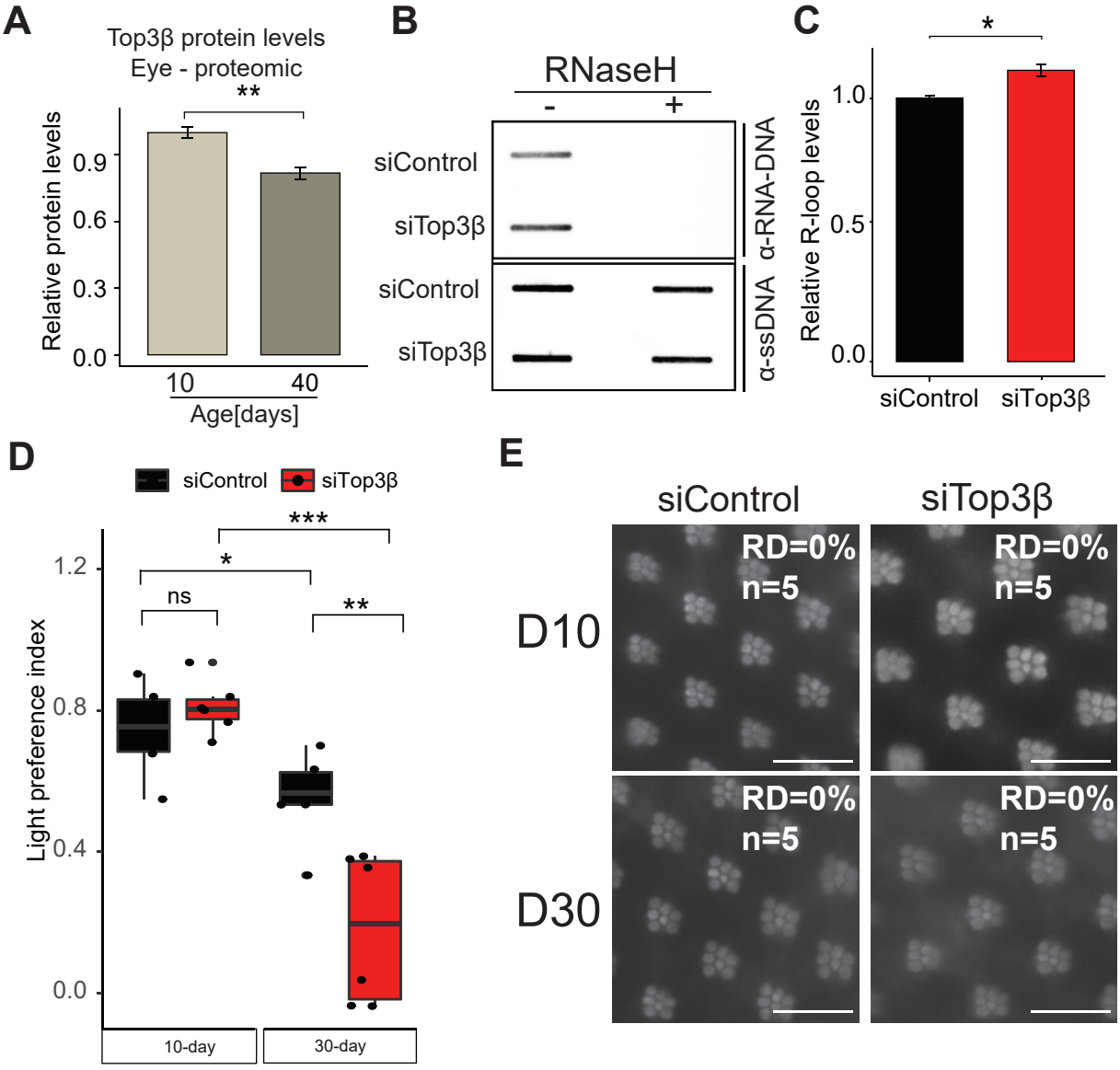
A
Top3β protein levels
Eye - proteomic
**
Relative protein levels
0.9
0.6
0.3
0.0
10
40
Age[days]
B
RNaseH
-
+
siControl
siTop3β
siControl
siTop3β
α-RNA-DNA
α-ssDNA
C
*
Relative R-loop levels
1.0
0.5
0.0
siControl
siTop3β
D
siControl
siTop3β
***
*
ns
**
Light preference index
1.2
0.8
0.4
0.0
10-day
30-day
E
siControl
siTop3β
D10
D30
RD=0%
n=5
RD=0%
n=5
RD=0%
n=5
RD=0%
n=5

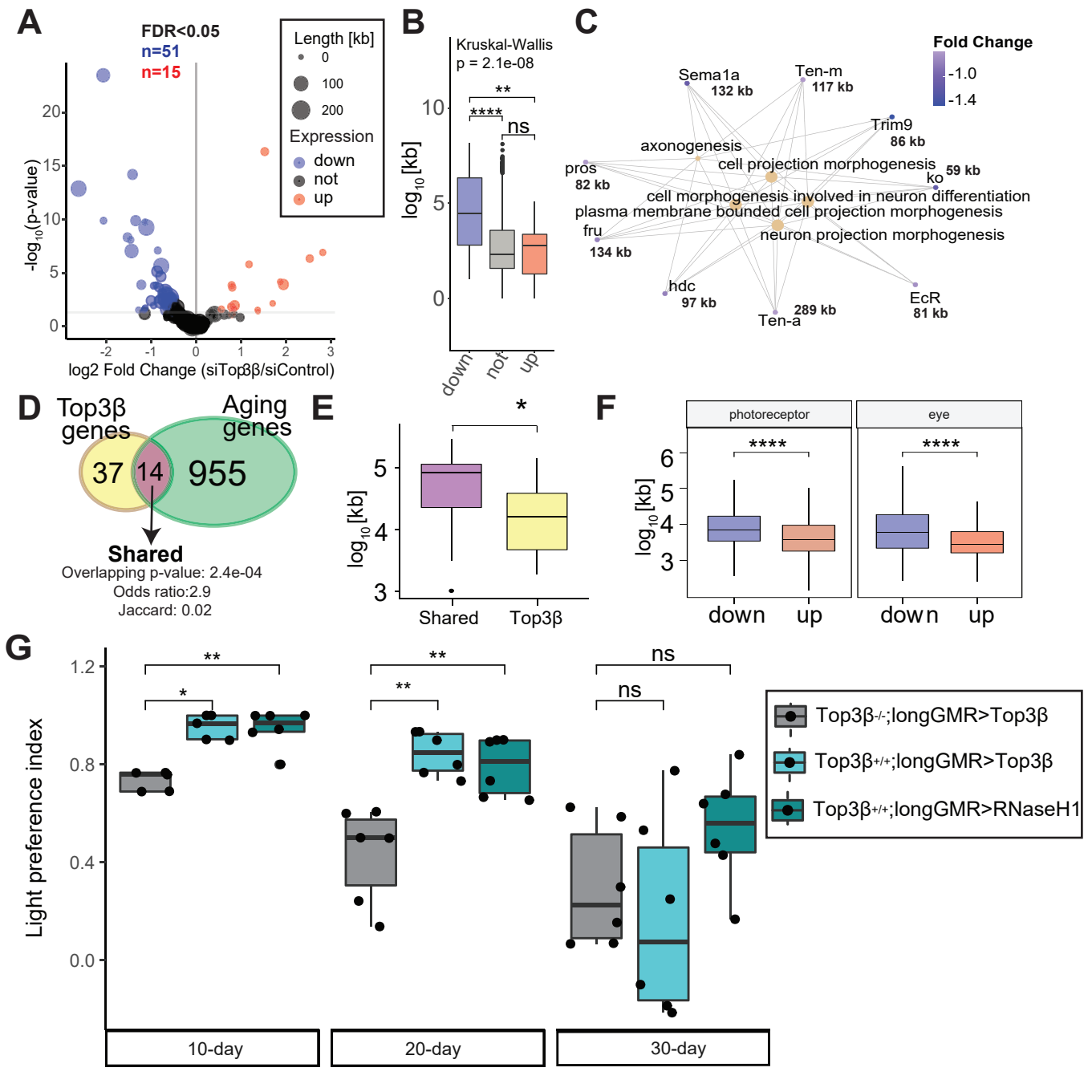
A
FDR<0.05
n=51
n=15
Length [kb]
0
100
200
Expression
down
not
up
-log10(p-value)
log2 Fold Change (siTop3β/siControl)
B
Kruskal-Wallis
p = 2.1e-08
log10[kb]
down
not
up
C
Fold Change
-1.0
-1.4
Sema1a
132 kb
Ten-m
117 kb
Trim9
86 kb
axonogenesis
cell projection morphogenesis
pros
82 kb
ko
59 kb
cell morphogenesis involved in neuron differentiation
plasma membrane bounded cell projection morphogenesis
fru
134 kb
neuron projection morphogenesis
hdc
97 kb
Ten-a
289 kb
EcR
81 kb
D
Top3β genes
Aging genes
37
14
955
Shared
Overlapping p-value: 2.4e-04
Odds ratio:2.9
Jaccard: 0.02
E
log10[kb]
Shared
Top3β
F
photoreceptor
eye
log10[kb]
down
up
down
up
G
Light preference index
10-day
20-day
30-day
Top3β-/-;longGMR>Top3β
Top3β+/+;longGMR>Top3β
Top3β+/+;longGMR>RNaseH1